

**Detection of massive forming galaxies  
at redshifts greater than one**

Lennox L. Cowie, Esther M. Hu & Antoinette Songaila

Institute for Astronomy, University of Hawaii, 2680 Woodlawn Dr., Honolulu, HI 96822

Accepted for publication in *Nature*

arXiv:astro-ph/9510045v1 8 Oct 1995

The complex problem of when and how galaxies formed has not until recently been susceptible of direct attack. It has been known for some time that the excessive number of blue galaxies counted at faint magnitudes<sup>1–5</sup> implies that a considerable fraction of the massive star formation in the universe occurred at  $z < 3$ ,<sup>6,7</sup> but, surprisingly, spectroscopic studies<sup>8–11</sup> of galaxies down to a  $B$  (blue) magnitude of 24 found little sign of the expected high- $z$  progenitors of current massive galaxies, but rather, in large part, small blue galaxies at modest redshifts ( $z \sim 0.3$ ). This unexpected population has diverted attention from the possibility that early massive star-forming galaxies might also be found in the faint blue excess. From our first spectroscopic observations deep enough to encompass a large population of  $z > 1$  field galaxies, we can now show directly that in fact these forming galaxies are present in substantial numbers at  $B \sim 24$ , and that the era from redshifts 1 to 2 was clearly a major period of galaxy formation. These  $z > 1$  galaxies have very unusual morphologies.

The recent availability of the highly sensitive multi-object Low Resolution Imaging Spectrograph (LRIS) on the Keck 10 m telescope on Mauna Kea, Hawaii has allowed us to extend and deepen quite considerably our spectroscopic coverage of the faint sky, and we are currently carrying out a redshift survey of faint galaxies using this instrument. The sample will consist of all objects satisfying the conditions  $K < 20$  or  $I < 22.5$  or  $B < 24.5$  in four  $6' \times 2'$  fields; so far, the most complete are those surrounding the Hawaii deep field SSA13<sup>4,12</sup> in which 147 of the 174 objects have been observed and 124 of these securely identified, and around SSA22, with 186 of the 193 objects observed and 157 identified. In all, ninety-one galaxies lying beyond  $z = 0.7$  and forty beyond  $z = 1$  have been identified in these two fields, with the highest redshift being  $z = 1.69$ . We show (Fig. 1) representative spectra of four galaxies at  $z > 1$ . Only three of the  $z > 0.7$  sample are galaxies with active nuclei (AGN). Most of the high redshift identifications are based on the presence of a strong

[O II] 3727 Å emission line (a nebular emission line of singly ionized oxygen) and weak Mg II 2800 Å absorption.<sup>11</sup> The general form of the spectra is illustrated in more detail in Fig. 2, which is the average of all the  $z > 0.7$  spectra in SSA13, excluding only the AGN. The composite spectrum closely resembles that of local blue galaxies<sup>13–15</sup> with very strong [O II] 3727, H $\beta$  and [O III] 5007, 4959 emission lines in the optical, and UV absorption lines of Fe II, Mn II and Mg II that confirm the [O II] redshift identification. These absorption lines in the composite spectrum are redshifted by an average of 300 km s<sup>-1</sup> from the emission lines, and may arise from gas infalling into the galaxy.

The [O II] 3727 emission lines in the high-redshift objects are remarkably strong (rest equivalent width of 60 Å in the composite spectrum) given that these are luminous galaxies with absolute rest  $B$  magnitudes of about  $-21$  for  $H_0=50$  km s<sup>-1</sup> Mpc<sup>-1</sup> and  $q_0=0.5$ . The [O II] luminosities ( $L_{[\text{O II}]}$ ) of the individual galaxies in the two fields are shown in Fig. 3(a), and we have also shown as crosses the [O II] luminosities for the Hawaii  $K \leq 19$  sample.<sup>16</sup> At low redshift ( $z < 0.7$ ) there are no galaxies in either sample with  $L_{[\text{O II}]} > 10^{42}$  ergs s<sup>-1</sup> while at  $z > 0.7$  there are 27 objects identified in these two fields. It is important to note that it is much easier to recognize and measure redshifts for objects with strong [O II] and there may be  $z > 1$  objects with lower [O II] luminosities hidden in the unidentified objects. There may also be additional objects at these redshifts lying beyond the magnitude limits of the present sample or among the remaining unobserved objects. This means the sample is not complete, but the key point is that even in this incomplete sample there is already a very large surface density of luminous star-forming galaxies.

To quantify this we must translate the [O II] luminosities into galaxy formation rates. This is discussed by Gallagher *et al.*<sup>17</sup> and by Kennicutt,<sup>18</sup> who point out that the [O II] line, though a more indirect calibrator than the unobserved H $\alpha$ , does provide a useful estimate

of the star formation rate, expressed in solar masses ( $M_{\odot}$ ) per year as:

$$\dot{M} (M_{\odot} \text{ yr}^{-1}) = 10^{-41} \alpha L_{[\text{O II}]} (\text{ergs s}^{-1}). \quad (1)$$

We have introduced the parameter  $\alpha$  to reflect the significant uncertainties in  $[\text{O II}]/\text{H}\alpha$  ratios, internal extinction, and the assumed stellar initial mass function (IMF). Gallagher *et al.* find  $\alpha = 1$  based on a sample of nearby blue galaxies while Kennicutt finds  $\alpha = 5$  for a wider sample of types. This range of values is a good measure of the uncertainty but the lower Gallagher *et al.* value may be more representative of the present sample, which is extremely blue.

For  $H_0=50 \text{ km s}^{-1} \text{ Mpc}^{-1}$  and  $q_0=0.5$ , as assumed in Fig. 3, the age of the universe at  $z = 1$  is  $6 \times 10^9 h^{-1} \text{ yrs}$  ( $h = H_0/50 \text{ km s}^{-1} \text{ Mpc}^{-1}$ ) and formation of a ‘normal’ galaxy with  $6 \times 10^{10} h^{-1} M_{\odot}$  of stars (a so-called  $L_*$  galaxy) would require a continuous star formation rate of  $10 M_{\odot} \text{ yr}^{-1}$ , corresponding to  $L_{[\text{O II}]} = 10^{42} \text{ ergs s}^{-1}$  for  $\alpha = 1$  (the dashed line in Fig. 3(a)). We note again that such galaxies are not seen at  $z < 0.7$  in the field samples (Fig. 2) nor in either of the local<sup>17,18</sup> samples, but are extremely common at  $z > 0.7$ . However, star formation need not proceed at a uniform rate in any individual galaxy, so the present observations might be picking out only the small subsample of starbursting galaxies at these redshifts. The best way to resolve this is to consider the volume production rate of  $[\text{O II}]$  photons by the ensemble of galaxies and compare this to the present mass density of stars in galaxies. This ensemble production rate of  $[\text{O II}]$  or  $\text{H}\alpha$  line photons directly measures the rate of massive star production and so can be linked immediately to the present day density of metals<sup>6,7</sup> in the universe or, slightly more indirectly and subject to uncertainties in the IMF, to the present-day mass density of stars in the universe.

We first define the volume production rate of  $[\text{O II}]$  photons as

$$\mathcal{L}_{[\text{O II}]}(z) = \sum_{\Delta z} \frac{L_{[\text{O II}]}}{V_{\Delta z}} \quad (2)$$

where the sum is over all galaxies lying in the redshift interval  $\Delta z$  surrounding  $z$ , and  $V_{\Delta z}$  is the comoving volume corresponding to the observed area. *De facto* we are restricted in the summation to observed, identified galaxies and our measured values are lower bounds, with the correction being larger at high  $z$ .  $\mathcal{L}_{[\text{O II}]}(z)$ , which can be converted directly to a stellar mass density formation rate using equation (1), is shown in Fig. 3(b) for redshift intervals from  $z = 0.25$  to 1.5. (It scales as  $h$ .) We have distinguished entries for SSA13 (boxes) and SSA22 (diamonds) to give some feeling for the uncertainty, but evidently the total rate of (massive) star formation was much higher in the recent past: even without any further correction for missing objects the star formation rate at  $z = 1.125$  was four times higher than that at  $z = 0.375$ .

Turning to absolute values, we can compare the measured star formation rates with that required to form the presently observed star density. For reference purposes we assume that the current stellar mass density is  $3 \times 10^8 h^2 \text{ M}_{\odot} \text{ Mpc}^{-3}$  and that the available time is  $17 h^{-1} (1+z)^{-3/2} \text{ Gyr}$ . To form the current stars at some period then requires a star formation rate,

$$\dot{\mu}_{ref} = 1.7 \times 10^{-2} (1+z)^{3/2} h^3 \text{ M}_{\odot} \text{ Mpc}^{-3} \text{ yr}^{-1}. \quad (3)$$

This reference rate is shown as the dashed and dotted lines in Fig. 3(b), which are computed for the values  $\alpha = 1$  and  $\alpha = 5$  respectively in equation 1. At  $z > 1$ , even in this quite incomplete sample, we are already seeing between 4% and 20% of the total galaxy formation.

Most of the luminous [O II] galaxies and most of the identified  $z > 1$  galaxies are drawn from objects with blue optical colors  $[(B - I) \leq 1.7]$  but relatively red infrared colors<sup>12</sup>  $[(I - K) \geq 1.8]$  (Fig. 4). Eleven of the sixteen objects in SSA13 with  $L_{[\text{O II}]} \geq 10^{42} \text{ ergs s}^{-1}$  and thirteen of the twenty objects with  $z > 1$  lie in this portion of the color-color plane; conversely nearly all the identified objects in this region are predominantly [O II]-luminous high- $z$  galaxies. Of the 18 objects identified in these regions two are AGN and two are low- $z$

galaxies but all those remaining have  $L_{[\text{O II}]} > 4 \times 10^{41}$  ergs s<sup>-1</sup> and lie at  $z > 0.7$ . Inspection of the color-color plane suggests that nearly all the low- $z$  galaxies in the sample have been identified and the remaining unidentified or unobserved objects are luminous high- $z$  star formers. Completion of the sample should therefore increase the  $z > 1$  galaxy formation rate substantially, bringing the measured mass rate much closer to the reference value.

Finally we have used deep  $I$ -band images, obtained with the wide field camera (WFPC2) on the Hubble Space Telescope (HST), of the central regions of the SSA13 and SSA22 fields<sup>19</sup> to investigate the morphologies of the high- $z$  starbursters. The images of all nine known objects in the HST fields with  $z > 1$  and  $L_{[\text{O II}]} \geq 10^{42}$  ergs s<sup>-1</sup> are shown in Fig. 5. Unlike lower redshift objects with high [O II] equivalent widths<sup>20</sup> the objects have strikingly unusual morphologies, often consisting of chains<sup>19</sup> or structures of compact blobs, suggesting that they are generally not dominated by uniformly distributed star formation. Recent studies have shown<sup>19,21</sup> that the excess galaxy counts at faint blue magnitudes are dominated by these anomalous galaxies and that at faint infrared magnitudes ( $K > 20$ ) these also become the single largest population.<sup>19</sup> Combined with the present results we can now recognize that forming galaxies enter the galaxy counts in substantial numbers at faint ( $B > 24$ ,  $K > 20$ ) magnitudes.

## REFERENCES

1. Kron, R. *Astrophys. J. Suppl. Ser.* **43**, 305–3 (1980)
2. Koo, D. *Astrophys. J.* **311**, 651–6 (1986)
3. Tyson, J. A. *Astr. J.* **96**, 1–23 (1988)
4. Lilly, S. J., Cowie, L. L. & Gardner, J. P. *Astrophys. J.* **369**, 79–105 (1991)
5. Metcalfe, N., Shanks, T., Fong, R. & Roche, N. *Mon. Not. R. astr. Soc.* **273**, 257–276 (1995)
6. Cowie, L. L. *The Post-Recombination Universe*, eds. Kaiser, N. & Lasenby, A. N., 1–18 (1988)
7. Songaila, A., Cowie, L. L. & Lilly, S. J. *Astrophys. J.* **348**, 371–377 (1990)
8. Broadhurst, T. J., Ellis, R. S. & Shanks, T. *Mon. Not. R. astr. Soc.* **235**, 827–856 (1988)
9. Colless, M., Ellis, R. S., Taylor, K. & Hook, R. N. *Mon. Not. R. astr. Soc.* **244**, 408–423 (1990)
10. Cowie, L. L., Songaila, A. & Hu, E. M. *Nature* **354**, 460–461 (1991)
11. Glazebrook, K., Ellis, R., Colless, M., Broadhurst, T., Allington-Smith, J. & Tanvir, N. *Mon. Not. R. astr. Soc.* **273**, 157–168 (1995) [astro-ph/9503116]
12. Cowie, L. L., Gardner, J. P., Hu, E. M., Songaila, A., Hodapp, K.-W. & Wainscoat, R. *J. Astrophys. J.* **434**, 114–127 (1994)
13. Rosa, M., Joubert, M. & Benvenuti, P. *Astr. Astrophys. Suppl. Ser.* **57**, 361–384 (1984)
14. Lamb, S. A., Gallagher, J. S., Hjellming, M. S. & Hunter, D. A. *Astrophys. J.* **291**, 63–71 (1985)

15. York, D. G., Caulet, A., Rybski, P., Gallagher, J., Blades, J. C., Morton, D. C. & Wamsteker, W. *Astrophys. J.* **351**, 412–7 (1990)
16. Songaila, A., Cowie, L. L., Hu, E. M. & Gardner, J. P. *Astrophys. J. Suppl. Ser.* **94**, 461–515 (1994)
17. Gallagher, J. S., Bushouse, H. & Hunter, D. A. *Astr. J.* **97**, 700–707 (1989)
18. Kennicutt, R. C. *Astrophys. J.* **388**, 310–327 (1992)
19. Cowie, L. L., Hu, E. M. & Songaila, A. *Astr. J.* **110**, 1576–1583 (1995)[astro-ph/9507055]
20. Colless, M., Schade, D., Broadhurst, T. J. & Ellis, R. S. *Mon. Not. R. astr. Soc.* **267**, 1108–1120 (1994) [astro-ph/9401028]
21. Glazebrook, K., Ellis, R., Santiago, B. & Griffiths, R. *Mon. Not. R. astr. Soc.* **275**, L19–L22 (1995) [astro-ph/9503101]

We would like to thank K. Glazebrook for a critical reading of a first draft of this manuscript and M. Colless, J. Cohen, J. Gallagher, O. LeFèvre and R. Williams for comments on the final version. We are grateful to T. Bida, P. Gillingham, J. Aycock, T. Chelminiak and W. Wack for their extensive help in obtaining the observations, which would not have been possible without J. Cohen and B. Oke’s LRIS spectrograph. The authors were visiting astronomers at the W. M. Keck Observatory, jointly operated by the California Institute of Technology and the University of California. This work was partly based on observations with the NASA/ESA *Hubble Space Telescope* obtained at the Space Telescope Science Institute, which is operated by AURA, Inc., under NASA contract. The research was supported at the University of Hawaii by the State of Hawaii and by NASA.



## FIGURES

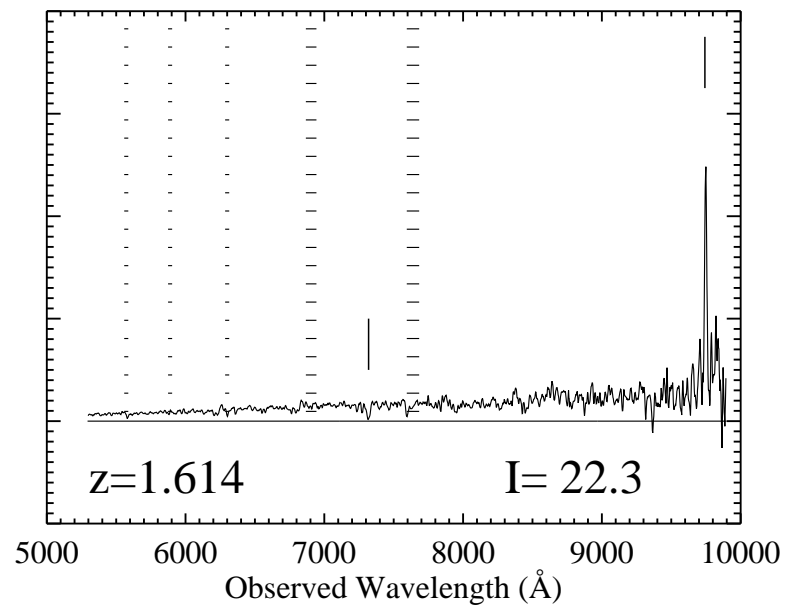
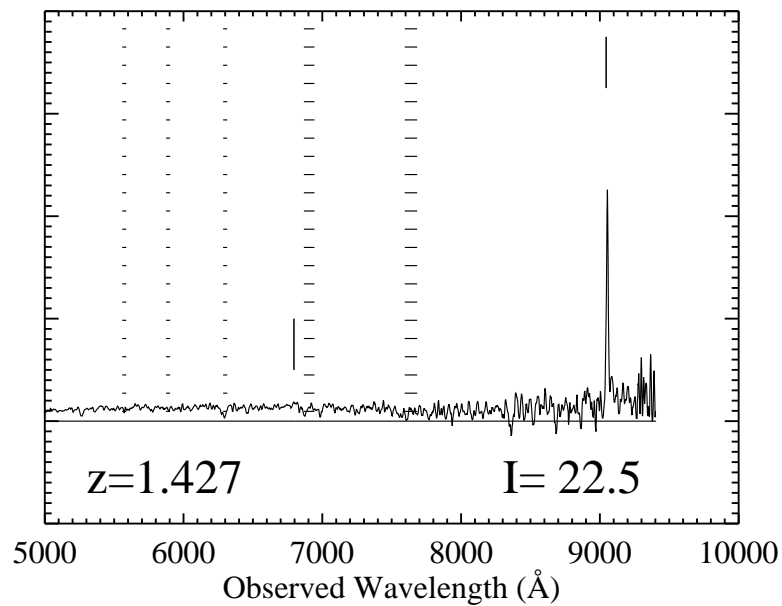
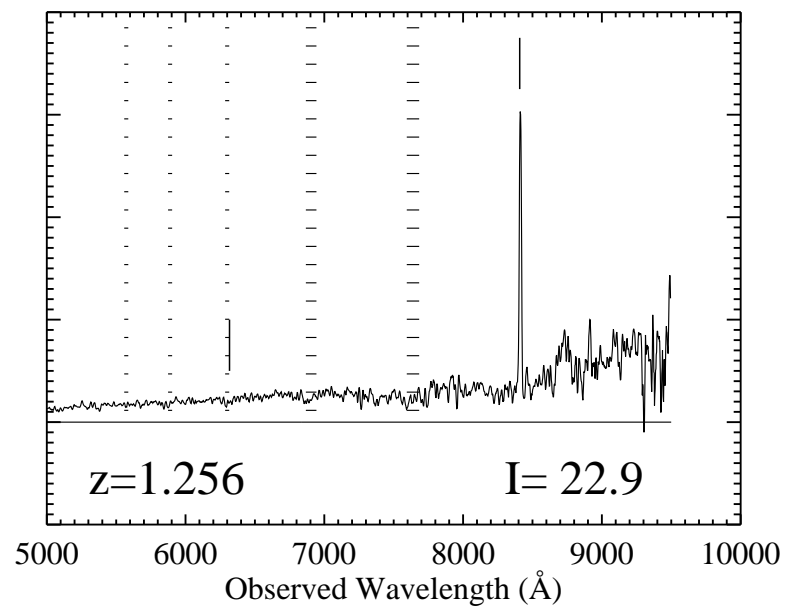
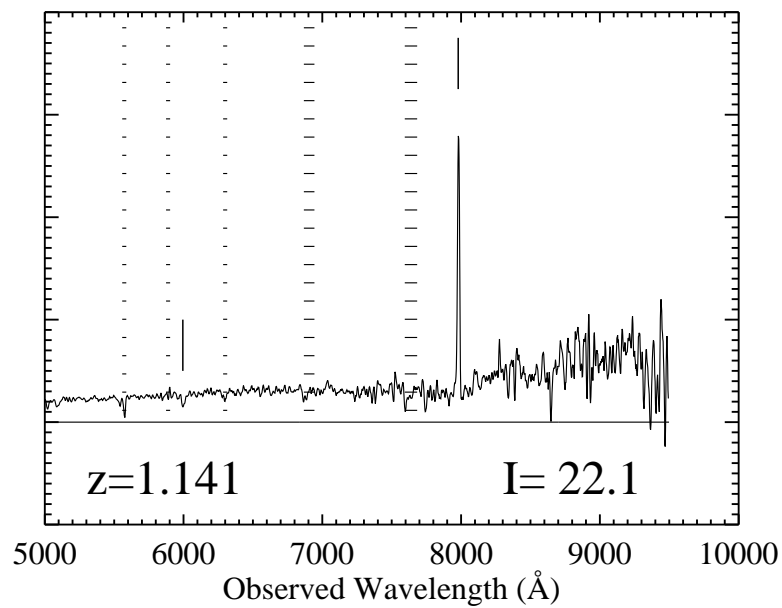
Fig. 1.— Sample spectra of  $z > 1$  galaxies observed with LRIS on the Keck 10 m telescope. Each object was observed with a  $1''.4$  wide slit using the  $300\ell/\text{mm}$  grating giving a resolution of  $17 \text{ \AA}$  and a wavelength coverage of  $5000 \text{ \AA}$ . Exposure times range from one to four hours. Each object is shown as  $f_\nu$  versus observed wavelength with the shaded regions showing the positions of strong night sky lines and atmospheric absorption bands. The tick marks show the position of Mg II  $2800 \text{ \AA}$  absorption and [O II]  $3727 \text{ \AA}$  emission at the redshift shown in the lower left corner. The apparent Kron-Cousins  $I$  magnitude is shown at the lower right.

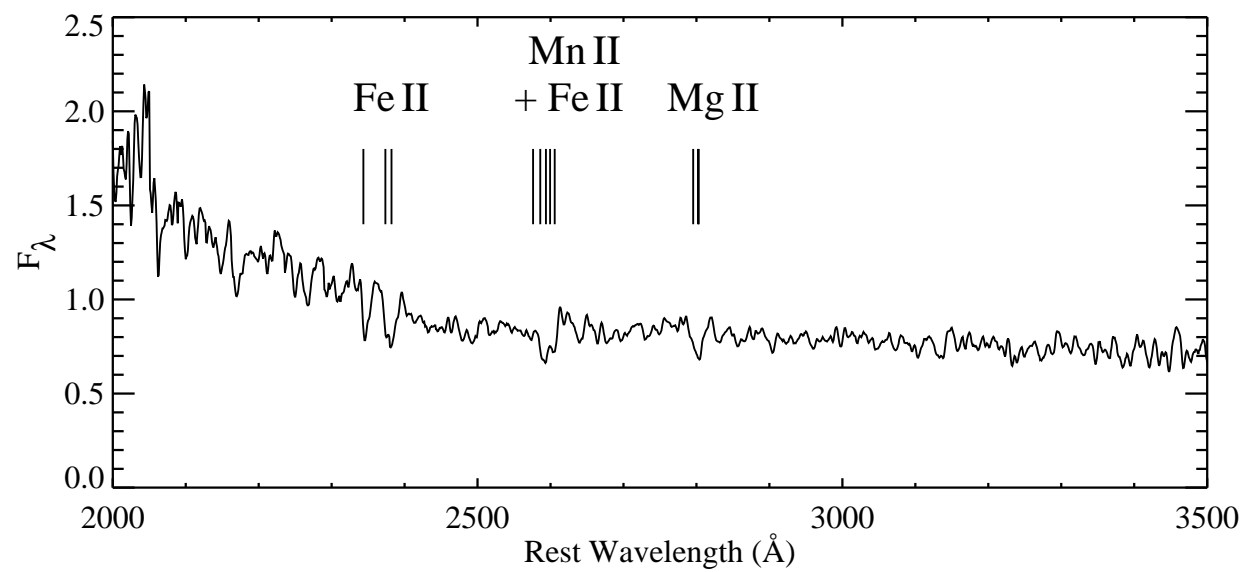
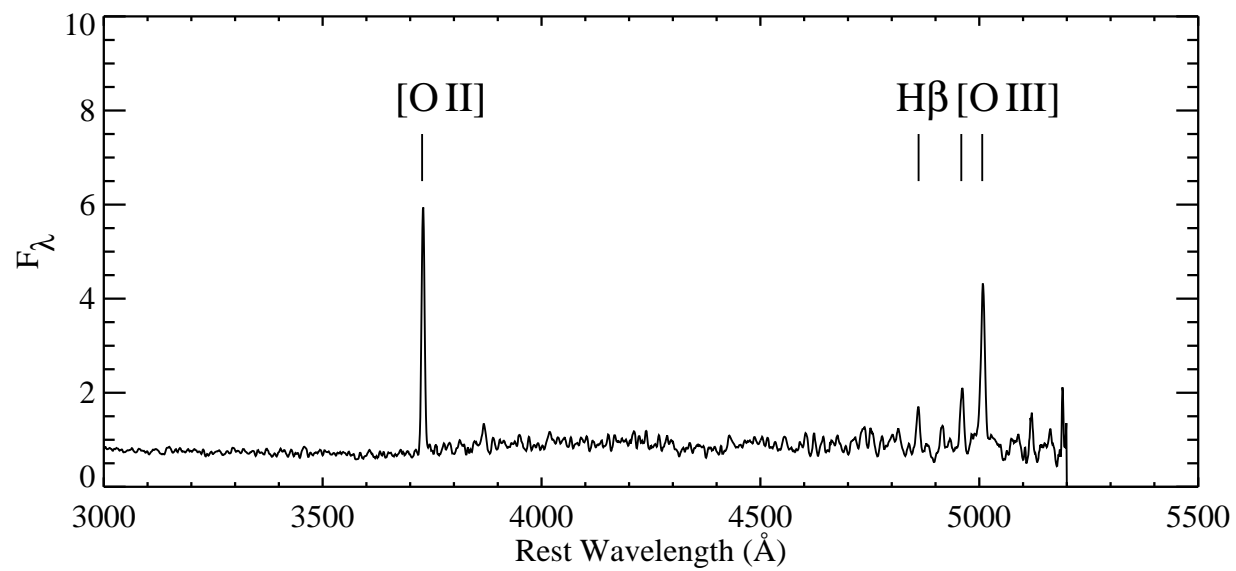
Fig. 2.— The average rest wavelength spectrum of objects with  $z > 0.7$  in the SSA13 field (excluding AGN). This composite spectrum was formed by normalizing all the spectra to their median value and then averaging all the spectra that covered a particular wavelength region. The optical portion of the spectrum is characterized by strong emission lines but only weak absorption lines are seen in the UV.

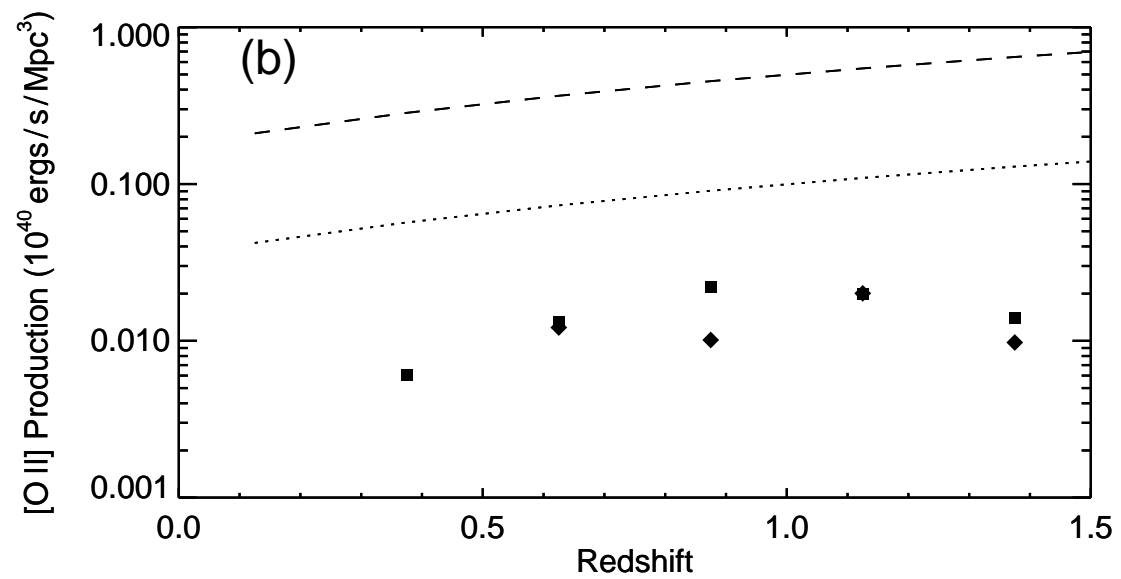
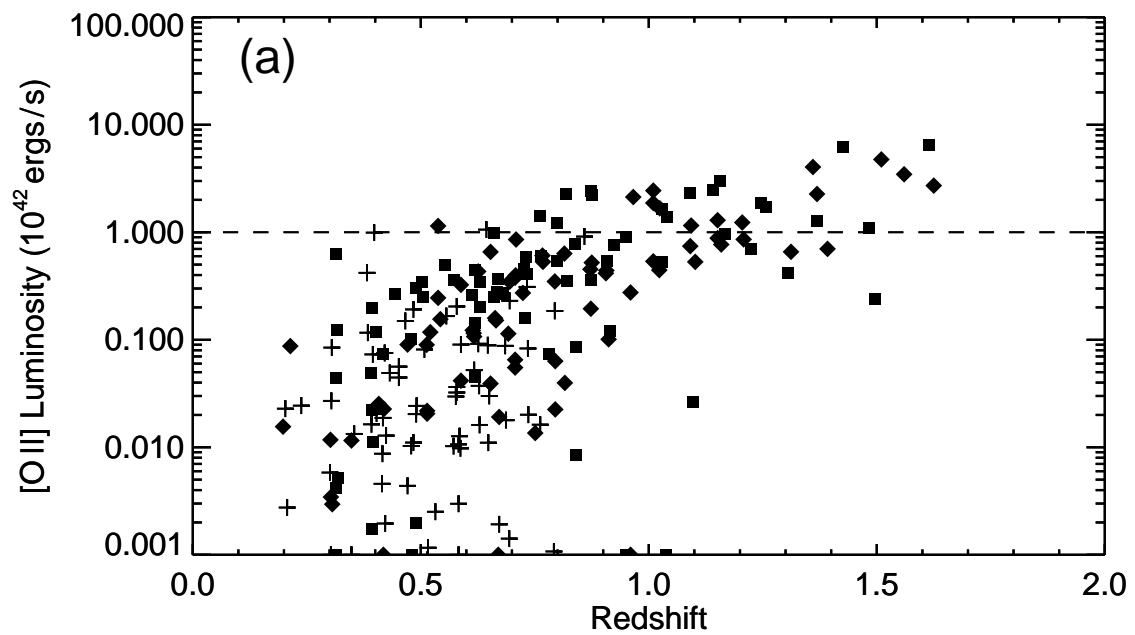
Fig. 3.— (a) The [O II] luminosities of galaxies in the SSA13 field (boxes) and SSA22 field (diamonds), computed by normalizing each spectrum to the flux in the measured broad-band magnitude nearest to the redshifted [O II] line to determine the continuum flux per unit wavelength,  $f_\lambda$  and combining this with the luminosity distance at redshift  $z$ . The Songaila *et al.* (1995) sample are also shown as crosses. The dashed line roughly divides rapidly forming galaxies from quiescent ones. No rapidly forming objects are seen at  $z < 0.7$  but they become very common at higher redshift. (b) The observed volume production rate of [O II] ( $\mathcal{L}_{[\text{O II}]}$ ) as a function of redshift for SSA13 (boxes) and SSA22 (diamonds) compared to the values required to form the present day galaxy population. The dashed line corresponds to Gallagher *et al.*'s<sup>17</sup> calibration of star formation rate versus [O II] luminosity and the dotted line to Kennicutt's.<sup>18</sup> Some measure of the uncertainties can be obtained by comparing the two fields.

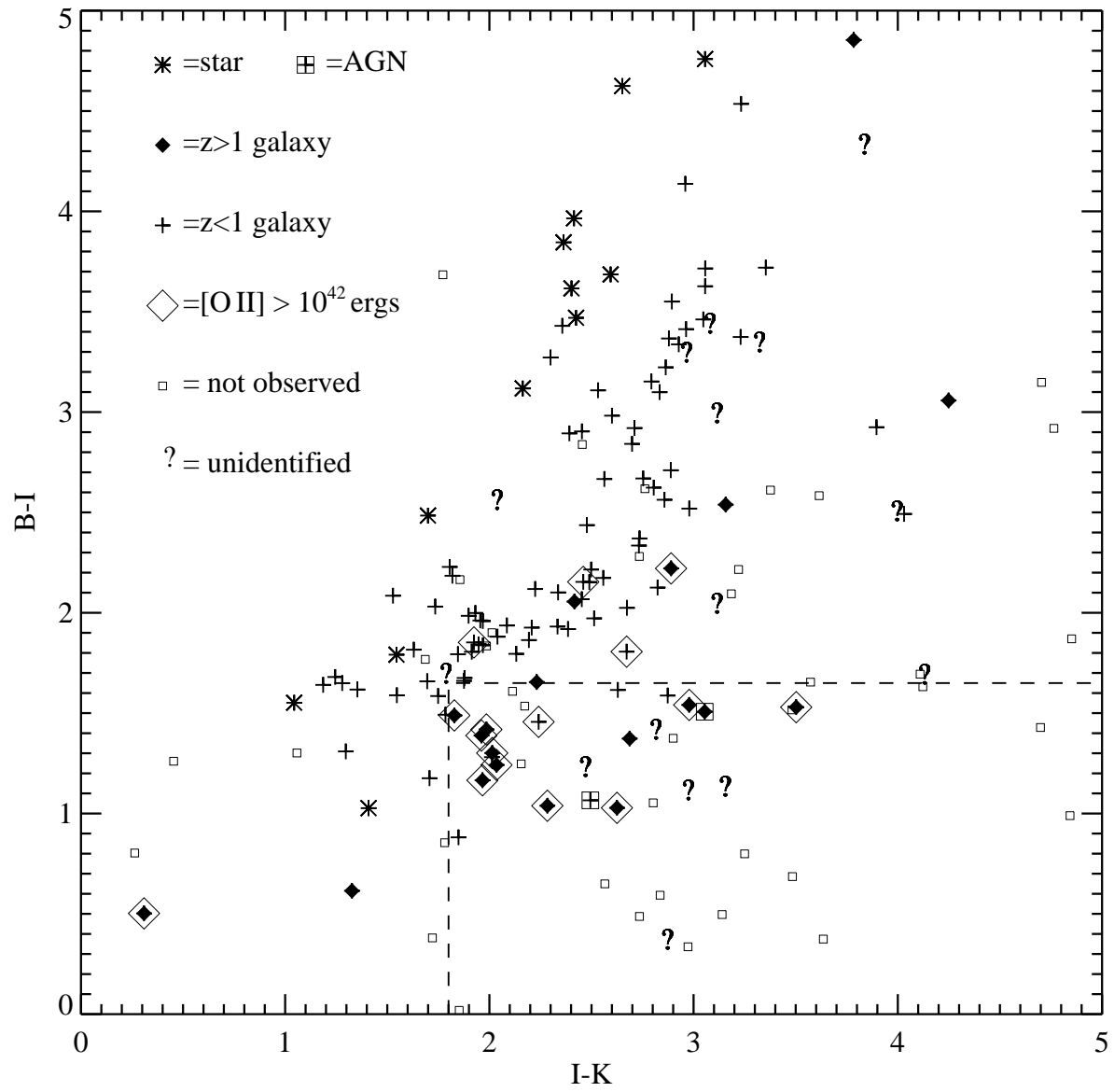
Fig. 4.— All the 174 magnitude-selected objects in the SSA13 field are shown in the  $(B - I)$  versus  $(I - K)$  color-color plane. The dashed rectangle shows the portion of the color-color plane where most of the high- $z$  [O II]-luminous galaxies are found. Many of the unidentified and most of the unobserved galaxies also lie in this region of color-color space.

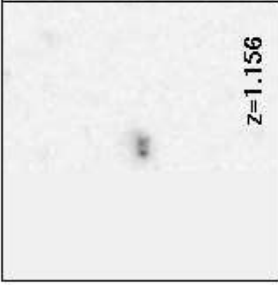
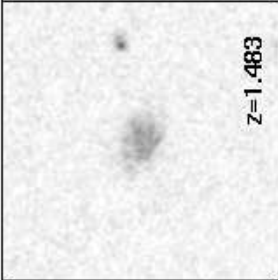
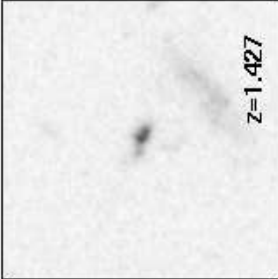
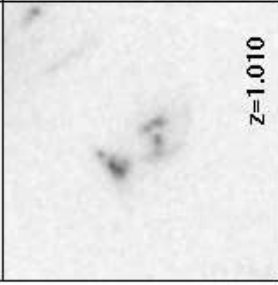
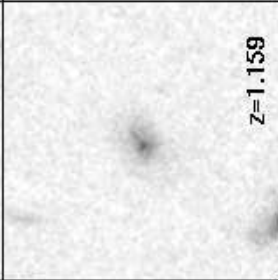
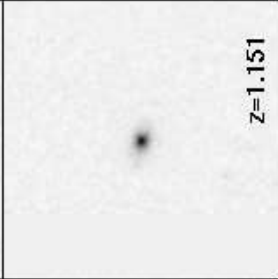
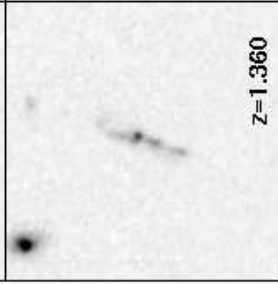
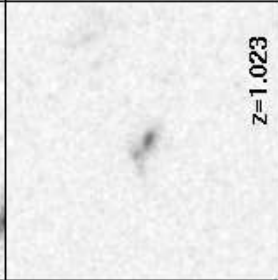
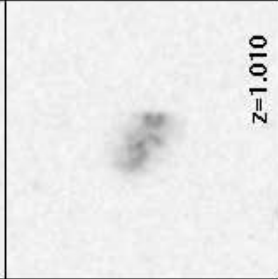
Fig. 5.— Deep HST  $I$ -band images from ref. 19 of all nine galaxies with  $z > 1$  and  $L_{[\text{O II}]} \geq 10^{42}$  ergs  $\text{s}^{-1}$  that lie in the HST fields. The boxes are  $8''$  on a side and the redshift of each object is shown in the lower right corner.









 <p><math>z=1.156</math></p>	 <p><math>z=1.483</math></p>	 <p><math>z=1.427</math></p>
 <p><math>z=1.010</math></p>	 <p><math>z=1.159</math></p>	 <p><math>z=1.151</math></p>
 <p><math>z=1.360</math></p>	 <p><math>z=1.023</math></p>	 <p><math>z=1.010</math></p>